Stairway to the Conical Intersection: A Computational Study of the Retinal Isomerization

ARTICLE *in* THE JOURNAL OF PHYSICAL CHEMISTRY A · OCTOBER 2007

Impact Factor: 2.69 · DOI: 10.1021/jp073908l · Source: PubMed

2 AUTHORS, INCLUDING:

Dage Sundholm
University of Helsinki

205 PUBLICATIONS **4,627** CITATIONS

SEE PROFILE

ARTICLES

Stairway to the Conical Intersection: A Computational Study of the Retinal Isomerization

Robert Send

Institut für Physikalische Chemie, Universität Karlsruhe, Kaiserstrasse 12, D-76128 Karlsruhe, Germany

Dage Sundholm*

Department of Chemistry, P.O. Box 55 (A.I. Virtanens plats 1), FI-00014 University of Helsinki, Finland

Received: May 21, 2007; In Final Form: July 9, 2007

The potential-energy surface of the first excited state of the 11-*cis*-retinal protonated Schiff base (PSB11) chromophore has been studied at the density functional theory (DFT) level using the time-dependent perturbation theory approach (TDDFT) in combination with Becke's three-parameter hybrid functional (B3LYP). The potential-energy curves for torsion motions around single and double bonds of the first excited state have also been studied at the coupled-cluster approximate singles and doubles (CC2) level. The corresponding potential-energy curves for the ground state have been calculated at the B3LYP DFT and second-order Møller−Plesset (MP2) levels. The TDDFT study suggests that the electronic excitation initiates a turn of the β-ionone ring around the C_6−C_7 bond. The torsion is propagating along the retinyl chain toward the cis to trans isomerization center at the C_{11}=C_{12} double bond. The torsion twist of the C_{10}−C_{11} single bond leads to a significant reduction in the deexcitation energy indicating that a conical intersection is being reached by an almost barrierless rotation around the C_{10}−C_{11} single bond. The energy released when passing the conical intersection can assist the subsequent cis to trans isomerization of the C_{11}=C_{12} double bond. The CC2 calculations also show that the torsion barrier for the twist of the retinyl C_{10}−C_{11} single bond adjacent to the isomerization center almost vanishes for the excited state. Because of the reduced torsion barriers of the single bonds, the retinyl chain can easily deform in the excited state. Thus, the CC2 and TDDFT calculations suggest similar reaction pathways on the potential-energy surface of the excited state leading toward the conical intersection and resulting in a cis to trans isomerization of the retinal chromophore. According to the CC2 calculations the cis to trans isomerization mechanism does not involve any significant torsion motion of the β-ionone ring.

I. Introduction

The photochemical isomerization reaction of retinal chromophores takes place in the femtosecond regime.[1,2] Experimental information about the evolution of the excitation wave packet and the structural dynamics must therefore be obtained by spectroscopical studies using femtosecond laser pulses. Femtosecond vibrational spectroscopy provides structural information about the molecule as a function of time, that is, it gives an understanding about the reaction pathway. For photoreactions, Raman spectroscopy is a very powerful tool since the electronic excitation initiates vibrational dynamics in the vicinity of the reaction center of the photoabsorbing chromophore where the reaction occurs, without significantly affecting the surrounding protein and the less photoactive parts of the chromophore. Mathies et al. have developed a femtosecond-stimulated Raman spectroscopy (FSRS) method and applied it in studies of the photoreaction dynamics of retinal chromophores in the visual pigment rhodopsin.[3−5] Atkinson et al. used in their retinal studies a different femtosecond vibrational spectroscopy technique denoted coherent anti-Stokes Raman scattering (CARS).[6,7]

Femtosecond time resolution of the photoreaction dynamics can also be deduced from Fourier transformed optical absorption (FTOA) spectra.[8] By using FTOA spectroscopy, Akiyama et al. suggested three main reaction steps in the isomerization mechanism of rhodopsin and bacteriorhodopsin.[9,10] They found that the initial step is completely temperature and isotopomer independent and that it occurs within 20 fs.[8−10] Thus, it can most likely be assigned to Franck−Condon (FC) relaxation. The dynamics of the second phase of the reaction is only slightly dependent on isotope substitutions at the C_{11}=C_{12} double bond where the cis to trans isomerization of rhodopsin takes place, whereas the third reaction phase indeed involves the isomerization center.[10] The FTOA measurements yielded qualitative information about the reaction steps in the femtosecond regime. However, no details about the changes in the molecular structure in the three reaction steps could be obtained from the FTOA experiments.

Atkinson et al. found in their picosecond time-resolved coherent anti-Stokes Raman spectroscopy PTR/CARS studies on bacteriorhodopsin pigments that the trans to cis isomerization

* To whom correspondence should be addressed. E-mail: sundholm@chem.helsinki.fi. Fax: +358-9-19150169. Phone: +358-9-19150176.

10.1021/jp073908l CCC: $37.00
Published on Web 08/22/2007

step does not occur immediately after the photoexcitation but happens at a later stage.[7] They found that the J-625 intermediate formed within 500 fs after the excitation has an all trans but nonplanar structure of the retinyl chain, whereas the isomerization has occurred for the K-590 intermediate 3 ps after the excitation.[7,11]

In recent FSRS studies by Mathies et al., a very similar mechanism was obtained for the photoisomerization reaction in rhodopsin.[4] They found that the reaction dynamics in this case can also be characterized by a three-step mechanism where the initial FC relaxation is followed by a fast evolution of the excited-state wave packet along the phase-space orbit of displaced FC coupled modes. The evolution is driven by the relaxation along the carbon−carbon single- and double-bond stretches and by the methyl rocking vibrations toward an excited-state equilibrium structure. Thus, the isomerization reaction mechanisms of rhodopsin and bacteriorhodopsin seem to be similar. In their FSRS study, Mathies et al. found that the nontotally symmetric modes such as hydrogen-out-of-plane (HOOP) modes and carbon backbone torsions are not excited in the initial absorption. These modes are excited 200−300 fs after the absorption by intramolecular vibrational energy redistribution from the displaced modes. The third step of the reaction mechanism involving atomic rearrangements and leading to the photo-isomerization surprisingly occurs on the ground-state potential-energy surface;[3] the conical intersection along the reaction pathway is reached before the double bond at the isomerization center is activated.

We have recently studied the gas-phase FC relaxation of the 11-*cis* retinal protonated Schiff base chromophore (PSB11) in the first excited state at the time-dependent density functional theory (TDDFT) and approximate singles and doubles coupled-cluster (CC2) level.[12,13] In these studies, the FC relaxation does not show the bond length inversion found in recent CASSCF and CASPT2 studies.[14,15] The differences in the molecular structures obtained at different levels of theory have been discussed in our recent studies.[12,13]

Here, we try to shed some light on the reaction mechanism of the photo isomerization by studying the structural changes in initial reaction steps of the isomerization of PSB11 by employing density functional theory (DFT) calculations. The changes in the molecular structure upon photoexcitation are calculated at the TDDFT level. The present studies refer to the PSB11 in the gas phase. They therefore provide little basis for comparison to the previously proposed isomerization mechanisms in the protein binding pocket such as the bicycle pedal or hula-twist motion.[16−18]

In this work, we focus on the second reaction step following the FC relaxation. The present reaction step is studied by analyzing three key reaction coordinates: (1) the $C_5{=}C_6{-}C_7{=}C_8$ torsion angle denoted ϕ, twisting the β-ionone ring; (2) the $C_9{=}C_{10}{-}C_{11}{=}C_{12}$ torsion angle denoted θ, twisting the single bond adjacent to the isomerization center; and (3) the $C_{10}{-}C_{11}{=}C_{12}{-}C_{13}$ torsion angle denoted γ, twisting the double bond at the isomerization center.

The coordinates ϕ and γ are analyzed by optimizing all internal coordinates while keeping ϕ or γ fixed. The coordinate θ is analyzed by single-point calculations while all other internal coordinates are fixed at the value of the relaxed ground state structure. The results of the present work are structured as follows. In section III A, the optimized structures of the ground and excited states are discussed. In section III B, the reaction coordinate ϕ, predominant in the FC relaxation, is analyzed. It is shown that the energy barrier for the coordinate θ vanishes for specific values of ϕ. In section III C, the coordinate θ that leads to a conical intersection is analyzed. In section III D, we analyze the coordinate γ along which the cis to trans isomerization eventually takes place. In sections III A−III D, the DFT and TDDFT calculations are compared to single-point MP2 and CC2 calculations along the same reaction coordinate. In section III E, the results are compared to those obtained in recent CASSCF and CASPT2 calculations.

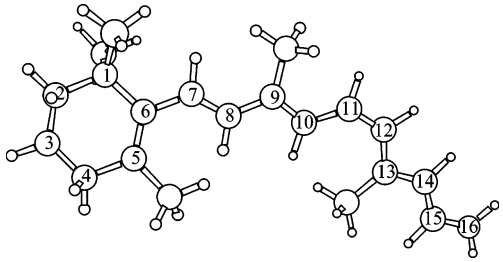

Figure 1. The enumeration of the skeleton carbon and nitrogen (16) atoms in the PSB11 chromophore.

II. Computational Methods

The molecular structure of the ground state of the 11-*cis* retinal protonated Schiff base (PSB11) was optimized at the DFT level using Becke's three-parameter hybrid functional[19] with the Lee−Yang−Parr correlation functional[20] (B3LYP). The molecular structure optimization of the first excited state of the PSB11 chromophore yielding the molecular changes due to the Franck−Condon relaxation was performed at the time-dependent density functional theory (TDDFT)[21−23] level also employing the B3LYP functional. The molecular structures were confirmed to be energy minima by calculating the harmonic vibrational frequencies using numerical differences. In the B3LYP calculations, the Karlsruhe triple-ζ basis sets augmented with one set of polarization functions (TZVP) were used.[24,25]

In the search for a conical intersection, the potential-energy surface for the first excited state was calculated at the B3LYP TDDFT level as a function of the torsion angle ϕ ($C_5{=}C_6{-}C_7{=}C_8$). In these calculations, all internal structural degrees of freedom except ϕ were fully optimized. Total and excitation energies for the first excited state were likewise calculated for given values of γ ($C_{10}{-}C_{11}{=}C_{12}{-}C_{13}$). In these calculations, the remaining internal coordinates were fully optimized. A similar procedure at the B3LYP DFT level was used in the calculation of the potential-energy curves for the ground state. For given values of θ ($C_9{=}C_{10}{-}C_{11}{=}C_{12}$), the total and excitation energies for the first excited state were determined in single-point calculations using the DFT ground-state structure as starting geometry. In these single-point calculations the remaining coordinates were kept fixed. The numbering of the atoms is shown in Figure 1.

The molecular structure of the ground state of the PSB11 chromophore was also optimized at the resolution-of-the-identity (RI) second-order Møller−Plesset perturbation theory (MP2) level using the new Karlsruhe triple-ζ quality basis sets augmented with two sets of polarization functions (def2-TZVPP).[26−28] The molecular structure of the first excited state of PSB11 was optimized at the coupled-cluster approximate singles and doubles level (CC2)[29] using the RI method.[30] The potential-energy curves for torsion twists around selected single and double bonds were obtained by performing single-point MP2 and CC2 calculations. In these calculations, one torsion angle was varied, whereas the remaining internal coordinates were kept unaltered. In the single-point MP2 and CC2 calcula-

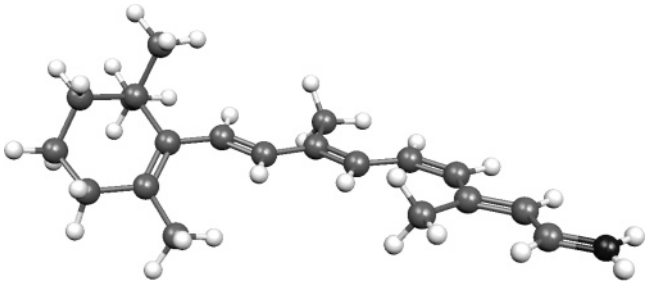

Figure 2. The molecular structure of the ground state of the PSB11 chromophore optimized at the B3LYP DFT level: $\phi = -39°$, $\theta = 178°$, $\gamma = -2°$.

tions, the def2-TZVP basis set was used which differs from def2-TZVPP by having only one set of polarization functions on the hydrogens. All calculations have been done with turbomole.[31]

The B3LYP DFT and TDDFT results presented in the following sections were validated by performing computationally more expensive CC2 calculations because it is known that TDDFT might have difficulties in treating states involving long-range charge transfer accurately.[32] The CC2 model might be more reliable than TDDFT because it should not suffer from any charge-transfer problems. On the other hand, it is not obvious that the electron correlation effects are considered accurately enough at the CC2 level. The method shows promise because the recent CC2 study on PSB11 employing large basis sets yielded excitation energies in close agreement with experimental values.[13]

III. Results

A. Structures. The molecular structure of the ground state of the retinal chromophore was optimized at the B3LYP DFT and MP2 levels. The B3LYP optimized structure is shown in Figure 2. At the B3LYP level, the retinyl chain is almost planar in the absence of the protein environment. All dihedral angles of the carbon backbone of the retinyl chain are close to 180° (0° at the cis position), whereas ϕ is −39°. At the MP2 level, ϕ is −45°. The ground-state structures optimized at the B3LYP and MP2 levels are largely identical.[12] The dihedral angles around the isomerization center at the C_{11}═C_{12} double bond show that the retinyl chain is somewhat more twisted at the MP2 level than obtained in the B3LYP optimization. The largest difference in the dihedral angles calculated at the MP2 and B3LYP levels is 15° which was obtained for γ.

For the molecular structure of the excited state optimized at the B3LYP TDDFT level, the β-ionone ring and the retinyl chain are perpendicular to each other with $\phi = -94°$.[12] The B3LYP TDDFT structure of the first excited state is shown in Figure 3. These results for the excited-state structure were supported by coupled-cluster calculations on retinal model compounds. For the 2-*cis*−$C_7H_8NH_2^+$ retinal model, the single bonds calculated at the B3LYP DFT/TDDFT and MP2/CC2 levels are longer for the excited state than for the ground state. This leads to a torsional twist of the single bond adjacent to the cis double bond. Coupled-cluster (CC2) optimization of the molecular structure of the first excited state of the retinal chromophore shows that the C_{10}−C_{11} single bond next to the isomerization center is the longest single bond in the retinyl chain for the first excited state, whereas at the B3LYP TDDFT level the C_6−C_7 single bond is the longest one leading to a torsional twist of the β-ionone ring relatively to the retinyl chain. However, at the CC2 level, we did not obtain any twist of the retinal single bonds for the retinal chromophore even though the single bonds

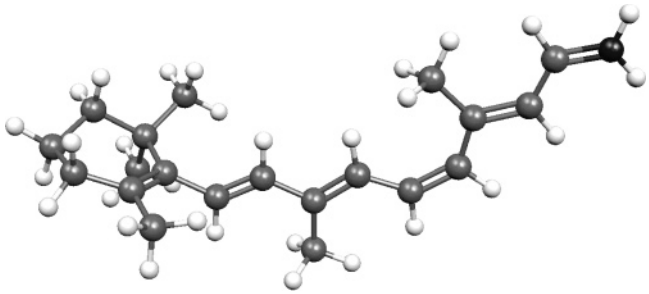

Figure 3. The molecular structure of the first excited state of the PSB11 chromophore optimized at the B3LYP TDDFT level: $\phi = -94°$, $\theta = 179°$, $\gamma = 0°$.

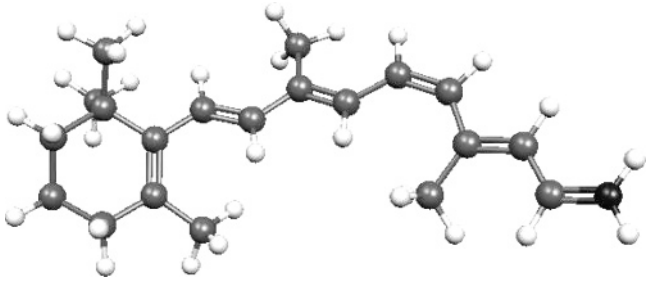

Figure 4. The molecular structure of the first excited state of the PSB11 chromophore optimized at the CC2 level: $\phi = -35°$, $\theta = -172°$, $\gamma = 10°$.

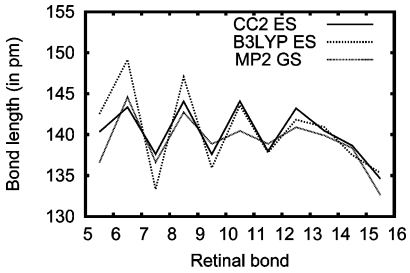

Figure 5. Comparison of the bond-length alternation of the C−C bonds of the excited state (ES) of the retinyl chain calculated at the B3LYP TDDFT and CC2 levels. The bond lengths for the ground state (GS) were obtained at the MP2 level. The bond length is given between the integers labeling the corresponding carbon atoms.

of the retinyl chain stretch and the double bonds shrink upon excitation. The molecular structure of the first excited state optimized at the CC2 level is shown in Figure 4. The bond-length alternation for the ground and first excited states calculated at the MP2, TDDFT, and CC2 levels are compared in Figure 5. Neither the B3LYP TDDFT nor the CC2 optimized structures for the first excited state show any indications of a cis to trans isomerization of the C_{11}═C_{12} bond. In a recent B3LYP DFT and TDDFT study, we found that the FC relaxation mainly activates a torsion twist around ϕ and a bond relaxation as indicated in Figure 5,[12] whereas the CC2 calculations suggest that the FC step activates only the C−C stretches of the retinyl chain. From a dynamic perspective, the C−C bond relaxation should be faster than the twist around ϕ. The atomic coordinates are given as Supporting Information.

B. The β-Ionone Ring Twist ϕ. The ground-state potential-energy curve for ϕ is shown in Figure 6. In the B3LYP DFT calculations, all internal coordinates except ϕ were fully optimized. Three minima were obtained on the potential-energy curve. The experimentally suggested structure of the retinal chromophore in rhodopsin corresponds to the B3LYP minimum at $\phi = -39°$. At the MP2 level, the corresponding minimum was obtained at $\phi = -45°$. These values can be compared to

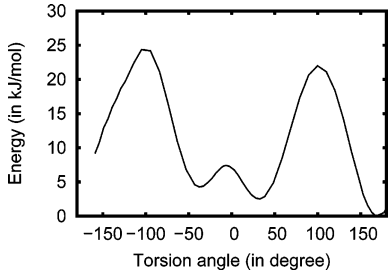

Figure 6. The ground-state potential-energy curve for the PSB11 chromophore as a function of the ϕ angle calculated at the B3LYP TDDFT level.

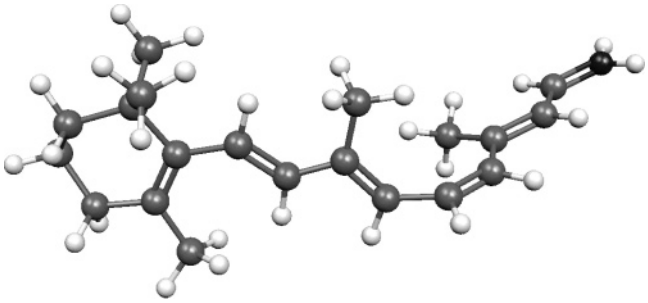

Figure 7. The molecular structure of the PSB11 chromophore in the vicinity of the conical intersection calculated at the B3LYP TDDFT level: $\phi = -4.2°$, $\theta = -90.3°$, $\gamma = 0.5°$.

the experimental values of $\phi = -30.3°$, $\phi = -31.9°$,[33] and $\phi = -44°$[34] for retinal embedded in the protein. At the DFT level, another minimum was obtained at $\phi = 33°$. The barrier between the two potential wells at $\phi = -39°$ and $\phi = 33°$ is 3−5 kJ/mol depending on the direction. This barrier corresponds to a temperature of only 380−580 K, which however is large enough to prevent a thermal change of the conformation in solution. The energetically lowest structure is located at $\phi = 167°$, and it is separated from the two other minima by an energy barrier of about 20 kJ/mol for the free chromophore. Such a high barrier prevents a thermal conformational change between them. The situation might be different for the rhodopsin chromophore because the relatively small barriers obtained for the free chromophore can be significantly altered by the presence of the surrounding protein. These aspects are discussed in a recent review.[35]

For the first excited state the situation is much more complicated. When the torsion angle ϕ is fixed at a given value and all internal coordinates except ϕ are optimized on the excited-state surface, there are two types of outcomes for the optimized structures: Type 1 has a geometry similar to that of the fully optimized excited-state structure described in section III A, differing mainly in ϕ; type 2 has a geometry with a highly twisted torsion angle θ close to $\theta = -90°$ and an almost vanishing gap between the highest occupied molecular orbital (HOMO) and the lowest unoccupied molecular orbital (LUMO) (see Figure 7).

In fact, for type 2 structures the HOMO−LUMO energy difference was too small for solving the Kohn−Sham equations, thus preventing the completion of the structure optimization. The potential-energy curve for type 1 geometries is shown in Figure 8a. The type 1 geometries were obtained by relaxing the structure of the excited state for ϕ values contained in the potential-energy curves with the equally deep minima at $\phi = 90°$ and $\phi = -94°$.

The type 2 geometries for the excited state were obtained when the initial ground-state structure has a ϕ angle between the vertical bars of Figure 8a. The vanishing HOMO−LUMO gap indicates a conical intersection. Even though the structure optimizations for type 2 geometries could not be completed because of the computational difficulties, the energy difference to the ground-state structure dropped to less than a tenth of the initial vertical excitation energy and the total energy is about half between the total energies of the ground and excited states calculated using the ground-state structure.

The excitation energy calculated as a function of ϕ is shown in Figure 8b where the conical intersection area is again indicated with vertical bars. It shows that the excitation energy is almost independent of ϕ angle when it lies in the [−125°, −50°] and [50°, 125°] intervals. However, it also shows that a large Stokes shift of about 1 eV is obtained for rather small changes in ϕ angle of about 10°. According to the DFT calculations, the vertical excitation of the retinal chromophore leads to a structure balancing on a sharp edge of the potential-energy curve in the first excited state. Structural relaxations toward larger torsion angles yield a minimum of the excited-state structure with a perpendicular orientation of the β-ionone ring, whereas a relaxation toward smaller torsion angles leads to the conical intersection. This could explain why the isomerization reaction is more efficient in the protein than in solution. The protein might adjust the dihedral angle ϕ to a slightly smaller value and thereby increase the probability for the relaxation toward the conical intersection resulting in a higher quantum yield for the retinal embedded in the protein than for the chromophore dissolved in, for example, methanol.

The CC2 potential-energy curve for the excited state with respect to the ϕ coordinate differs significantly from the TDDFT one. At the TDDFT level, the optimization of the first excited state leads to a perpendicular orientation of the ring with respect to the retinyl chain, whereas the CC2 optimization of the first excited state results in only a small change of 10° in ϕ as compared to the ground state. For the optimized CC2 structure, the ϕ angle is −35°. The CC2 single-point calculations of the potential-energy curve with respect to ϕ did not show any indications of a conical intersection, whereas the TDDFT optimizations yielded practically vanishing deexcitation energies for small ϕ angles. The potential-energy curves obtained in the single-point CC2 calculations are given in Figure 9. However, the CC2 potential-energy curve cannot directly be compared to the TDDFT one, because in the single-point CC2 calculations the remaining internal coordinates were unaltered. At the TDDFT level, the structure was reoptimized for each given value of ϕ. Secondary effects such as twists of other retinyl bonds cannot occur in single-point calculations. Note that the second excited state seems to have a minimum for the perpendicular orientation of the β-ionone ring at the CC2 level, that is, similarly as obtained for the first excited state in the TDDFT calculations.

C. The C_9=C_{10}−C_{11}=C_{12} Single Bond Twist θ. The B3LYP TDDFT calculations show that the restriction of the internal coordinate ϕ can lead to a torsional rotation around θ for certain values of ϕ. These structural changes are reminiscent of the FC relaxation mechanism obtained for the 2-*cis*−C_7H_8-NH_2^+ retinal model.[12] Because the twist around θ does not occur spontaneously in the FC relaxation step of the retinal it must be prevented by an energy barrier. The experimentally observed ultrafast dynamics indicates that the energy barriers are very low.[36−40] The height of the torsion barrier along the ϕ coordinate was calculated at the B3LYP TDDFT level. The potential-energy curves in Figure 10 were obtained for given values of θ. In the calculations, the remaining internal coordinates were kept fixed. Figure 10a shows that the potential curve of the ground state

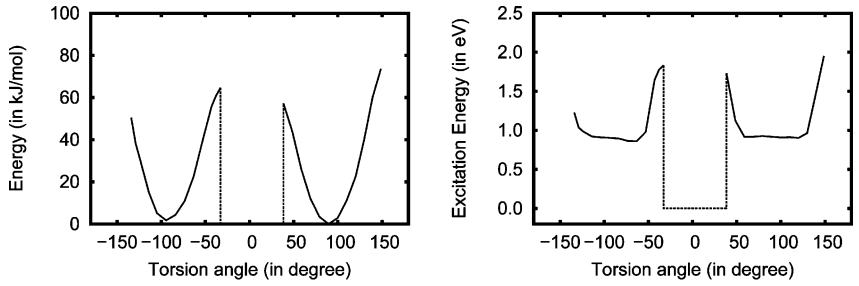

Figure 8. (a) The potential-energy curve and (b) the excitation energy for the first excited state of the PSB11 chromophore as a function of the ϕ angle calculated at the B3LYP TDDFT level.

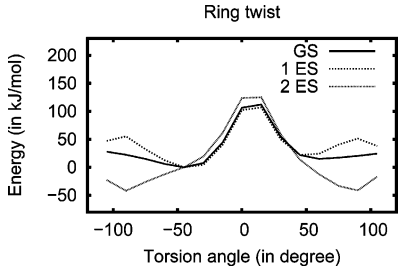

Figure 9. The CC2 potential curves as a function of the ϕ angle have been calculated for the three lowest states. The molecular structure of the ground state has been the starting geometry for the single-point CC2 calculations. The absolute energy scale of all states has been set to 0 kJ/mol at the MP2 ground-state minimum at $\phi = -45°$.

has a huge torsion barrier of more than 100 kJ/mol, whereas the corresponding potential curve for the excited states, also enlarged in Figure 10b, is very shallow with an energy barrier of about 10 kJ/mol. The corresponding B3LYP excitation energies are given as a function of θ in Figure 11. The graph shows that the B3LYP excitation energy decreases and approaches zero when rotating out of the plane along the θ coordinate.

The potential-energy curves calculated at the CC2 level given in Figure 12 show that the torsion barrier for rotations along θ is very small for the first excited state. The barrier is even smaller when the CC2 excited-state structure instead of the ground-state structure is used as the starting geometry in the single-point calculations. The energy barrier of about 4 kJ/mol is more than 1 order of magnitude smaller than that obtained for the ground state. The corresponding potential-energy barrier calculated at the B3LYP TDDFT level is about 10 kJ/mol. In this case, the TDDFT and CC2 calculations yield qualitatively the same result. For the ground state, the MP2 torsion barrier with respect to θ is about 75 kJ/mol as compared to the almost vanishing ones obtained for the first excited state.

In Figure 11, the CC2 excitation energies of the first and second excited states are also given as a function of θ. For the perpendicular orientation with torsion angles of about $\theta = \pm 90°$, the first excitation energy is significantly smaller than obtained for the ground-state structure. However, judged from the CC2 calculations it is not obvious that a conical intersection can be reached by twisting the C_{10}—C_{11} single bond. One should though bear in mind that single-point CC2 calculations might have problems in accurately describing the approach of a conical intersection.

D. The C_{10}—C_{11}═C_{12}—C_{13} Double Bond Twist γ. The photochemical reaction of the retinal chromophore results in a cis to trans isomerization, which is experimentally found to occur after the conical intersection has been reached.[4] These recent experimental results were investigated by calculating the torsion barrier as a function of the twist angle γ. The potential-energy curves shown in Figure 13 were obtained at the B3LYP DFT and TDDFT levels for the ground and first excited state, respectively. In the calculations, the remaining internal coordinates were fully optimized. The potential-energy curves with respect to γ show that the torsion barrier for the excited state is at least as high as for the ground state. The shape of the potential curves for the ground and excited state are identical for small torsion angles, indicating that the isomerization center is not activated at an early stage of the reaction. Thus, these computational results support the recent experimental findings that the C_{11}═C_{12} double bond is not involved in the initial reaction steps of the isomerization reaction.[4,7,8] The calculated torsion barriers are larger than 100 kJ/mol for both the ground and the excited states. That barrier is large enough to prevent the isomerization through a one-bond flip. This notion is also supported by recent X-ray measurements of the electron-density difference between rhodopsin and bathorhodopsin.[41] It should be noted that the exact shape and magnitude of the barrier is uncertain. Because of the difficulties of DFT and TDDFT methods to describe states with pronounced multireference character, it makes no sense to calculate the potential-energy curve with a better resolution around the energy maxima in Figure 13. The sparse grid of points leads to the sharp cusps in the potential-energy curves. However, the calculations indeed suggest that the isomerization does not occur immediately after the excitation.

The CC2 energy barriers for the twist along the γ angle are shown in Figure 14. The ground-state potential curves were obtained at the MP2 level. The CC2 and MP2 calculations show that for the first excited state the energy barrier for the γ twist is about 1 order of magnitude larger than for θ rotations. The energy barrier is somewhat higher when the excited-state structure is used as initial geometry in the single-point calculations than with the ground-state structure as starting point. At the B3LYP TDDFT level, the obtained energy barrier with respect to γ is around 100 kJ/mol, whereas the CC2 energy barrier is about a factor of 2 smaller. The large energy barrier of 50−100 kJ/mol prevents the torsion twist, that is, the isomerization of the C_{11}═C_{12} double bond for the excited state. The 50 kJ/mol reduction in the energy barrier for the double-bond twist of the excited state obtained at the CC2 level might be considered to be preliminaries for facilitating the isomerization step.

In Figure 15, the CC2 excitation-energy functions of the first and second excited states are compared to the B3LYP TDDFT

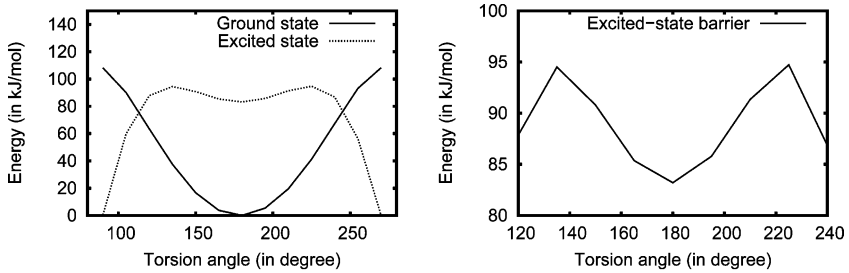

Figure 10. (a) The potential curve as a function of the θ angle calculated for PSB11 at the B3LYP DFT and B3LYP TDDFT levels for the ground and first excited state, respectively. The molecular structure of the ground state has been the starting point for the single-point B3LYP DFT and B3LYP TDDFT calculations. The absolute energy scale has been set to 0 kJ/mol at the lowest points of each, the ground and excited-state curve. (b) The potential curve of the excited state is zoomed in.

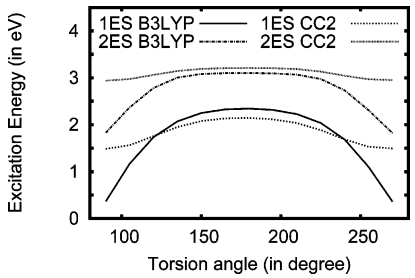

Figure 11. The excitation energy as a function of the θ twist angle for the PSB11 chromophore calculated at the B3LYP TDDFT and CC2 levels, respectively. The molecular structures of the ground state optimized at the B3LYP and MP2 levels have been the starting point for the single-point B3LYP TDDFT and CC2 calculations, respectively.

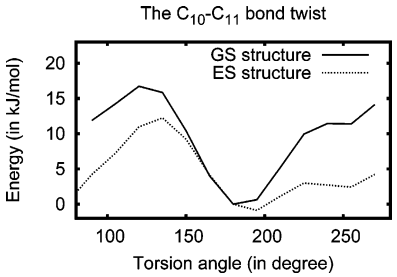

Figure 12. The potential-energy curve as a function of the θ angle calculated at the CC2 level. The molecular structures of the ground state (GS) and first excited state (ES) have been the starting point for the single-point CC2 calculations. The absolute energy scale of the ground- and excited-state curves has been set to 0 kJ/mol at the minimum of the ground-state curve.

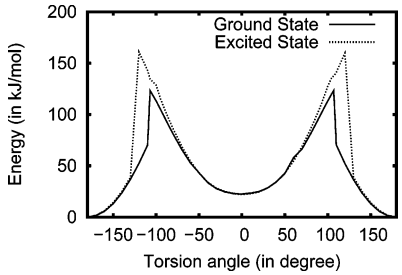

Figure 13. The potential-energy curves for the ground and first excited states of the PSB11 chromophore as a function of the γ angle calculated at the B3LYP DFT and TDDFT level. All internal coordinates other than γ have been fully optimized. The absolute energy scale has been set to 0 kJ/mol at the lowest points of each, the ground- and excited-state curve.

ones. The CC2 excitation-energy curves agree well with those obtained at the B3LYP TDDFT level. The excitation energies were calculated as a function of the γ angle with all remaining coordinates kept unchanged. For comparison, both the CC2 and the B3LYP TDDFT calculations in this graph have the MP2 ground-state structure as starting geometry.

E. Comparison of ab Initio and DFT Methods. Our recent CC2 calculations of the vertical excitation energies of the retinal chromophore yielded values of 2.10 and 3.17 eV for the two lowest excited states.[13] These energies are in good agreement with the recently measured gas-phase values of 2.03 and 3.18 eV.[42] The vertical excitation energy of 2.34 eV calculated at the B3LYP TDDFT level is thus 0.3 eV larger. The full B3LYP TDDFT optimization of the first excited state results in a large shift of 1.44 eV. Thus, the optimization of the excited-state structure reduces the vertical excitation energy by 0.9 eV,[12] whereas at the CC2 level the Stoke shift is 0.28 eV. The CC2 model has proven to be useful in studies of excited states insofar as large basis sets are employed.[43] The CC2 method is therefore used here to assess the reliability of the B3LYP TDDFT potential-energy surface of the first excited state of the retinal chromophore.

It has also been argued that the excitation process of retinals cannot be described at the TDDFT level[44] mainly because the results do not agree with those obtained at the complete active space self-consistent field (CASSCF) level in combination with multiconfiguration second-order perturbation theory (CASPT2) calculations.[45] However, a comparison of CASSCF/CASPT2 excitation energies with gas-phase data indicates shortcomings of the CASSCF/CASPT2 approach in retinal studies.[14] There might be several reasons for the difficulties of the CASSCF/CASPT2 method to describe the isomerization process.[14,46−51] First, the often employed 6-31G* basis set is indeed small for ab initio correlation calculations. Second, the more serious flaw in the CASSCF calculations on retinals is probably due to the necessary limitation of the active space to 12 electrons in 12 orbitals. The present CC2 calculation of the natural occupation numbers shows that the differences between the orbital occupation numbers are very small at the boundaries of the active space. According to the CC2 occupation numbers, it is not obvious why the 12-in-12 active space, on the basis of chemical intuition, should be large enough for an accurate or at least for a balanced treatment of the most important electron correlation effects. Most likely, more than 12 electrons in 12 orbitals have to be included in the active space to get an accurate molecular structure at the CASSCF level. In Figure 16, the orbital distribution function of the particle−hole occupation numbers is given. The natural orbitals obtained at the CC2 level are sorted according to descending occupation. The vertical lines denote the 12-in-12 active space. The occupation numbers for many of the orbitals outside the 12-orbital active space are of the same size as for those correlated at the 12-in-12 CASSCF level.

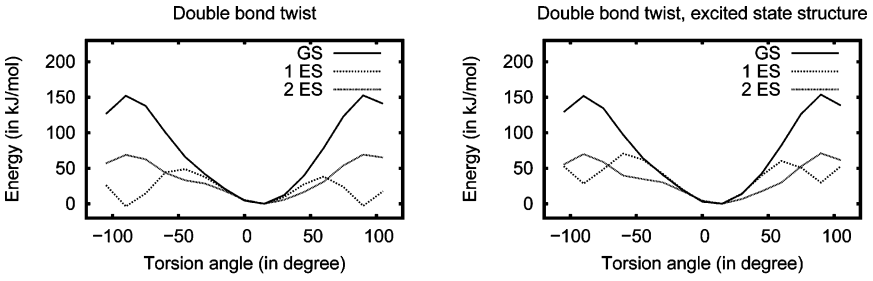

(a) (b)

Figure 14. The CC2 potential-energy curves as a function of the γ angle has been calculated for the three lowest states. (a) The molecular structure of the ground state (GS) has been the starting geometry for the single-point CC2 calculations. (b) The molecular structure of the first excited state has been the starting geometry for the single-point CC2 calculations. The absolute energy scale of the ground- and excited-state curves has been set to 0 kJ/mol at the minimum of the ground-state curve.

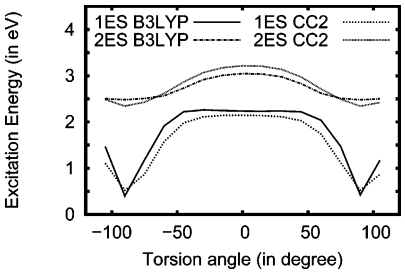

Figure 15. The excitation energy as a function of the γ angle for the PSB11 chromophore calculated at the B3LYP TDDFT and CC2 levels, respectively. The molecular structure of the ground state optimized at the MP2 level has been the starting point for the single-point B3LYP TDDFT and CC2 calculations.

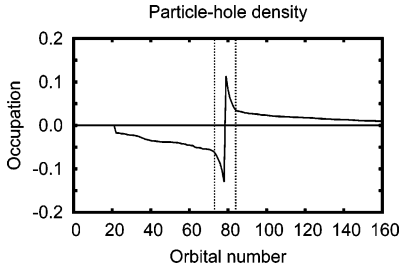

Figure 16. The particle−hole occupation numbers for the retinal chromophore calculated at the CC2 level.

The electron correlation effects omitted at the CASSCF level can be considered by performing CASPT2 calculations. However, the molecular structure optimized at the CASSCF level is usually adopted in the CASPT2 calculations. The CASPT2 calculation improves the treatment of the electron correlation, whereas single-point CASPT2 calculations cannot correct the errors introduced by the use of a less accurate CASSCF molecular structure. This holds especially when studying changes in molecular structures due to electronic excitation processes.

In a recent study, we found that the ground-state structure obtained at the CASSCF level differs significantly from the MP2 and B3LYP DFT structures suggesting that the limited size of the active space might introduce significant errors. In the CASSCF/CASPT2 study by Sekharan et al.,[49] the use of an atomic-natural-orbital (ANO) basis set in combination with an MP2 optimized molecular structure yielded a rather accurate value for the first excitation energy, whereas the second excitation energy was 0.34 eV too small as compared to the experiment.[42] A similar study using the CASSCF molecular structure[14] overestimated the two lowest excitation energies by 0.3 eV as compared to the recent gas-phase values.[42]

IV. Conclusions

The TDDFT calculations indicate that the photoreaction for the free chromophore begins with a Franck−Condon relaxation involving the β-ionone ring and the retinyl C−C stretches. Thus, the isomerization center at the C_{11}=C_{12} double bond is activated at a later stage. However, when the chromophore is embedded in the protein, steric effects might prevent the twist of the β-ionone ring relative to the retinyl chain. The single bonds stretch and the double bonds shrink upon excitation. The torsion barrier for the cis to trans isomerization of the C_{11}=C_{12} double bond of about 100 kJ/mol is about as large for the excited state as obtained for the ground state. The torsion barriers for the single-bond twist around the C_9=C_{10}−C_{11}=C_{12} (the θ torsion angle) practically vanishes. The twist around θ leads to a drastic reduction of the deexcitation energy indicating that a conical intersection is reached that way. When the conical intersection is being approached about half of the excitation energy has been made available for the isomerization step. The calculations suggest that the isomerization occurs after the conical intersection, that is, on the potential-energy surface of the ground state as also observed experimentally.[3]

The CC2 calculations roughly support the TDDFT results. At the CC2 level, the torsion barrier with respect to θ is less than 5 kJ/mol, which is even smaller than the energy barrier of 10 kJ/mol obtained at the TDDFT level. According to the CC2 calculations, the torsion barrier with respect to the rotation of the C_{10}−C_{11}=C_{12}−C_{13} torsion angle (the γ angle) is reduced by a factor of 2 for the excited state, but it is still very high preventing the isomerization on the excited-state potential-energy surface. Because of the reduced barriers, the retinyl chain can easily deform in the excited state as also observed experimentally.[3,7,36,52] The main difference between the B3LYP and CC2 reaction mechanisms is that the CC2 calculations suggest that the β-ionone ring plays an unobtrusive role, whereas according to the TDDFT calculations the β-ionone ring participates actively in the Franck−Condon relaxation step. The CC2 calculations on the other hand suggest that the FC step activates retinyl C−C stretches which from a dynamic perspective should also be faster than the twist of the β-ionone ring (the ϕ angle twist). The reaction step involving the β-ionone ring could though explain the significantly larger quantum yield obtained for the chromophore embedded in the protein. The enhanced quantum yield could either be due to steric interactions preventing the twist of ϕ or alternatively the protein lowers the torsion barrier for the twist around θ. The protein can also favor the trans structure when the reaction is passing the conical intersection. A combination of all these mechanisms is likely since they do not exclude each other.

Acknowledgment. This research has been supported by the Academy of Finland through its Centers of Excellence Programme 2006-2011. We acknowledge financial support from the European research training network on "Understanding Nanomaterials from a Quantum Perspective" (NANOQUANT), contract No. MRTN-CT-2003-506842, from the Nordisk Forskerakademi network for research and research training (NorFA Grant No. 030262) on "Quantum Modeling of Molecular Materials" (QMMM). Prof. Reinhart Ahlrichs (Karlsruhe) and Prof. Christof Hättig (Bochum) are thanked for up-to-date versions of the turbomole program package and the ricc2 program. We are grateful to Dr. Filipp Furche for helpful discussions, and CSC, the Finnish IT Center for Science, for computer time.

Supporting Information Available: Cartesian coordinates for the molecules. This material is available free of charge via the Internet at http://pubs.acs.org.

References and Notes

(1) Kandori, H.; Furutani, Y.; Nishimura, S.; Shichida, Y.; Chosrowjan, H.; Shibata, Y.; Mataga, N. *Chem. Phys. Lett.* **2001**, *334*, 271−276.
(2) Kandori, H.; Shichida, Y.; Yoshizawa, T. *Biochemistry (Moscow)* **2001**, *66*, 1197−1209.
(3) Kukura, P.; McCamant, D. W.; Yoon, S.; Wandschneider, D. B.; Mathies, R. A. *Science* **2005**, *310*, 1006−1009.
(4) McCamant, D. W.; Kukura, P.; Mathies, R. A. *J. Phys. Chem. B* **2005**, *109*, 10449−10457.
(5) Kukura, P.; Yoon, S.; Mathies, R. A. *Anal. Chem.* **2006**, *78*, 5952−5959.
(6) Atkinson, G. H.; Ujj, L.; Zhou, Y. *J. Phys. Chem. A* **2000**, *104*, 4130−4139.
(7) Terentis, A. C.; Ujj, L.; Abramczyk, H.; Atkinson, G. H. *Chem. Phys.* **2005**, *313*, 51−62.
(8) Akiyama, R.; Kakitani, T.; Imamoto, Y.; Shichida, Y.; Hatano, Y. *J. Phys. Chem.* **1995**, *99*, 7147−7153.
(9) Akiyama, R.; Yoshimori, A.; Kakitani, T.; Imamoto, Y.; Shichida, Y.; Hatano, Y. *J. Phys. Chem. A* **1997**, *101*, 412−417.
(10) Kakitani, T.; Akiyama, R.; Hatano, Y.; Imamoto, Y.; Shichida, Y.; Verdegem, P.; Lugtenburg, J. *J. Phys. Chem. B* **1998**, *102*, 1334−1339.
(11) Abramczyk, H. *J. Chem. Phys.* **2004**, *120*, 11120−11132.
(12) Send, R.; Sundholm, D. *J. Phys. Chem. A* **2007**, *111*, 27−33.
(13) Send, R.; Sundholm, D. *Phys. Chem. Chem. Phys.* **2007**, *9*, 2862−2867.
(14) Cembran, A.; González-Luque, R.; Altoè, P.; Merchán, M.; Bernardi, F.; Olivucci, M.; Garavelli, M. *J. Phys. Chem. A* **2005**, *109*, 6597−6605.
(15) Aquino, A. J. A.; Barbatti, M.; Lischka, H. *Chem. Phys. Chem.* **2006**, *7*, 2089−2096.
(16) Warshel, A. *Science* **1976**, *260*, 679−683.
(17) Liu, R. S. H.; Asato, A. E. *Proc. Natl. Acad. Sci. U.S.A.* **1985**, *82*, 259−263.
(18) Liu, R. S. H.; Hammond, G. S. *Chem. Eur. J.* **2001**, *7*, 4536−4544.
(19) Becke, A. D. *J. Chem. Phys.* **1993**, *98*, 5648−5652.
(20) Lee, C.; Yang, W.; Parr, R. G. *Phys. Rev. B* **1988**, *37*, 785−789.
(21) Bauernschmitt, R.; Ahlrichs, R. *Chem. Phys. Lett.* **1996**, *256*, 454−464.
(22) Furche, F.; Ahlrichs, R. *J. Chem. Phys.* **2002**, *117*, 7433−7447.
(23) Furche, F.; Ahlrichs, R. *J. Chem. Phys.* **2004**, *121*, 12772−12773.
(24) Schäfer, A.; Huber, C.; Ahlrichs, R. *J. Chem. Phys.* **1994**, *100*, 5829−5835.
(25) Weigend, F.; Häser, M.; Patzelt, H.; Ahlrichs, R. *Chem. Phys. Lett.* **1998**, *294*, 143−152.
(26) Weigend, F.; Häser, M. *Theoret. Chem. Acc.* **1997**, *97*, 331−340.
(27) Weigend, F.; Köhn, A.; Hättig, C. *J. Chem. Phys.* **2002**, *116*, 3175−3183.
(28) Weigend, F. *Phys. Chem. Chem. Phys.* **2006**, *8*, 1057−1065.
(29) Christiansen, O.; Koch, H.; Jørgensen, P. *Chem. Phys. Lett.* **1995**, *243*, 409−418.
(30) Hättig, C.; Weigend, F. *J. Chem. Phys.* **2000**, *113*, 5154−5161.
(31) Ahlrichs, R.; Bär, M.; Häser, M.; Horn, H.; Kölmel, C. *Chem. Phys. Lett.* **1989**, *162*, 165−169. For the current version, see: http://www.turbomole.de.
(32) Dreuw, A.; Head-Gordon, M. *Chem. Rev.* **2005**, *105*, 4009−4037.
(33) Okada, T.; Sugihara, M.; Bondar, A. N.; Elstner, M.; Entel, P.; Buss, V. *J. Mol. Biol.* **2004**, *342*, 571−583.
(34) Gascón, J. A.; Batista, V. S. *Biophys. J.* **2004**, *87*, 2931−2941.
(35) Gascón, J. A.; Sproviero, E. M.; Batista, V. S. *Acc. Chem. Res.* **2006**, *39*, 184−193.
(36) Schenkl, S.; van Mourik, F.; Friedman, N.; Sheves, M.; Schlesinger, R.; Haacke, S.; Chergui, M. *Proc. Natl. Acad. Sci. U.S.A.* **2006**, *103*, 4101−4106.
(37) Hasson, K. C.; Gai, F.; Anfinrud, P. A. *Proc. Natl. Acad. Sci. U.S.A.* **1996**, *93*, 15124−15129.
(38) Du, M.; Fleming, G. R. *Biophys. Chem.* **1993**, *48*, 101−111.
(39) Haran, G.; Wynne, K.; Xie, A. H.; He, Q.; Chance, M.; Hochstrasser, R. M. *Chem. Phys. Lett.* **1996**, *261*, 389−395.
(40) Gai, F.; Hasson, K. C.; Cooper McDonald, J.; Anfinrud, P. A. *Science* **1998**, *279*, 1886−1891.
(41) Nakamichi, H.; Okada, T. *Angew. Chem., Int. Ed.* **2006**, *45*, 4270−4273.
(42) Nielsen, I. B.; Lammich, L.; Andersen, L. H. *Phys. Rev. Lett.* **2006**, *96*, 018304.
(43) Lehtonen, O.; Sundholm, D. *J. Chem. Phys.* **2006**, *125*, 144314.
(44) Wanko, M.; Garavelli, M.; Bernardi, F.; Miehaus, T. A.; Frauenheim, T.; Elstner, M. *J. Chem. Phys.* **2004**, *120*, 1674−1692.
(45) Andersson, K.; Malmqvist, P. Å.; Roos, B. O. *J. Chem. Phys.* **1992**, *96*, 1218−1226.
(46) Ferré, N.; Olivucci, M. *J. Am. Chem. Soc.* **2003**, *125*, 6868−6869.
(47) Andruniów, T.; Ferré, N.; Olivucci, M. *Proc. Natl. Acad. Sci. U.S.A.* **2004**, *101*, 17908−17913.
(48) Cembran, A.; Bernardi, F.; Olivucci, M.; Garavelli, M. *Proc. Natl. Acad. Sci. U.S.A.* **2005**, *102*, 6255−6260.
(49) Sekharan, S.; Weingart, O.; Buss, V. *Biophys. J.* **2006**, *91*, L07−09L.
(50) Schreiber, M.; Sugihara, M.; Okada, T.; Buss, V. *Angew. Chem., Int. Ed.* **2006**, *45*, 4274−4277.
(51) Coto, P. B.; Strambi, A.; Ferre, N.; Olivucci, M. *Proc. Natl. Acad. Sci. U.S.A.* **2006**, *103*, 17154−17159.
(52) Kobayashi, T.; Saito, T.; Ohtani, H. *Nature* **2001**, *414*, 531−534.